BULLETIN OF THE POLISH ACADEMY OF SCIENCES
TECHNICAL SCIENCES, Vol. 71(4), 2023, Article number: e146107
DOI: 10.24425/bpasts.2023.146107

ARTIFICIAL AND COMPUTATIONAL INTELLIGENCE

Application of fuzzy type II multi-layer Kalman filter for parameters identification of two-mass drive system

Kacper ŚLESZYCKI[1]*, **Karol WRÓBEL**[1], **Krzysztof SZABAT**[1], and **Seiichiro KATSURA**[2]

[1] Wrocław University of Science and Technology, Institute of Electrical Machines, Drives and Measurements, Wrocław, Poland
[2] Keio University, Department of System Design Engineering, Tokyo, Japan

Abstract. The paper describes a novel online identification algorithm for a two-mass drive system. The multi-layer extended Kalman Filter (MKF) is proposed in the paper. The proposed estimator has two layers. In the first one, three single extended Kalman filters (EKF) are placed. In the second layer, based on the incoming signals from the first layer, the final states and parameters of the two-mass system are calculated. In the considered drive system, the stiffness coefficient of the elastic shaft and the time constant of the load machine is estimated. To improve the quality of estimated states, an additional system based on II types of fuzzy sets is proposed. The application of fuzzy MKF allows for a shorter identification time, as well as improves the accuracy of estimated parameters. The identified parameters of the two-mass system are used to calculate the coefficients of the implemented control structure. Theoretical considerations are supported by simulations and experimental tests.

Key words: electrical drives; torsional vibration; state estimation; Kalman filter; multi-layer estimator.

1. INTRODUCTION

Electrical motors are becoming increasingly popular in different industrial applications. They replace other types of actuators, such as pneumatic or hydraulic systems. This is due to their very favorable properties, such as high energy density, resistance to working conditions, ease of supply, and the ability to shape their characteristics (with the help of modern control methods) [1–7]. Industrial drives consist of several basic elements: a driving motor (with supply and control elements), a working machine, and a torque transmission part (e.g. belts, gearboxes, long shafts, chains). This complicated connection of the several parts generates torsional vibrations in the mechanical system [1–7]. To implement high-performance control of such mechanisms one of the advanced frameworks should be implemented [1–7]. To perform it, knowledge of the system parameters is necessary. The parameters of the driving motors can be obtained from the data sheets provided by the manufacturer. However, the parameters of the mechanical parts are often not accessible. Therefore, one of the identification methods should be implemented before the operation.

In the literature, there are plenty of different identification schemes that can be used for this task. In general, they can be divided into two main groups. The first one relay on the procedure running before normal operation [8–11]. In this case, the mechanical system is excited by special signals. Then the parameters of the plant are determined and the coefficients of the implemented control structure are computed. Methodologies evident in this group can be further divided into parametric [8] and non-parametric [9–14] methods. The first approach is based on the transfer function polynomial, and the second one is based on frequency characteristics. Because the identification procedure is performed before the normal operation of the drive, these frameworks are sometimes called also off-line identification methodologies.

The second group is based on the algorithms implemented online [15, 16]. It means that the algorithm is running all the time and provides the current values of the identified parameters. This can be treated as an advantage of this system. The estimated parameters can be used to implement an adaptive control structure or for condition monitoring purposes. The methodologies based on EKF are especially popular in this group [15, 16]. As drawbacks, the following features can be pointed out. Firstly, the complicated algorithm of EKF. Secondly, the difficulties of setting the covariance matrices **Q** and **R** in an industrial application (where the assumption about characters of noises is usually not fulfilled). Thirdly, the limited convergence speed of states in the EKF in the presence of unknown initial conditions of the systems or rapid (step) changes of plant states. This is especially important for the adaptive control system based on the identified parameters.

There are a lot of different control algorithms reported in the literature designated for damping mechanical oscillations. Because a simple PI controller cannot suppress torsional vibrations effectively [17], other frameworks have been proposed in the literature. One of the most popular is based on the insertion of additional feedback from selected state variables [18]. The next concepts are based on the implementation of disturbance observers [18–20]. The state controller, sliding mode, neural networks, or adaptive control structure should be also mentioned here [21–23]. One of the latest approaches, which has gained a lot of attention from the control community, relies

*e-mail: kacper.sleszycki@pwr.edu.pl

Manuscript submitted 2022-03-28, revised 2023-04-18, initially accepted for publication 2023-05-23, published in August 2023.

on model predictive control [24–27]. It should be underlined, that to implement the majority of advanced control strategies, knowledge of the plant parameters is obligatory.

Fuzzy logic systems are often used in modern control applications. They can replace the classical algorithm completely, or be used as an additional support system. In general, they are implemented in cases where the available knowledge of the system is limited and can be represented in the form of linguistic rules rather than algebraic equations. The firstly proposed fuzzy systems were based on type I fuzzy sets. In this approach, the shapes and locations of membership functions are exactly specified. Those requirements are hard to fulfill in some applications with a high level of uncertainty. Therefore, the system based on type II sets was introduced in the literature. In this approach, the boundary of membership functions is also fuzzed. The more complicated form of fuzzy sets ensures obtaining higher precision in the presence of uncertainty and limitation of available knowledge [28, 29].

In this paper, the issues related to the online identification procedure for a two-mass system are presented. The multi-layer EKF concept is used in the work [30–32]. The proposed estimator has two layers. In the first one, three single EKFs are placed to estimate values of the mechanical part of the drive (mechanical time constant of the load machines as well as stiffness time constant). In the second layer, an aggregation mechanism is implemented to calculate the states of the system. Contrary to [30], where basic results have been introduced, in the present work additional system is used to improve the quality of estimated states. It is based on fuzzy type II sets. The main role of this system is to detect the dynamic states of the plant, according to it, the estimation process is switched on or off. This allows for improving the quality of the estimation of all states. In addition, preliminary results showing the work of the adaptive control structure are presented in the paper. Moreover, results showing the advantage of multi-layer structure for the cases of improper values of EKF are presented. The theoretical consideration is supported by simulation and experimental results.

2. MATHEMATICAL MODEL OF THE PLANT AND CONTROL STRUCTURE

2.1. Mathematical model of the two-mass drive system

The mathematical model of the drive system with flexibility is given by the state equation [17]:

$$\frac{\mathrm{d}}{\mathrm{d}t}\begin{bmatrix}\omega_1(t)\\ \omega_2(t)\\ m_s(t)\end{bmatrix} = \begin{bmatrix}0 & 0 & \frac{-1}{T_1}\\ 0 & 0 & \frac{1}{T_2}\\ \frac{1}{T_c} & \frac{-1}{T_c} & 0\end{bmatrix}\begin{bmatrix}\omega_1(t)\\ \omega_2(t)\\ m_s(t)\end{bmatrix} + \begin{bmatrix}\frac{1}{T_1}\\ 0\\ 0\end{bmatrix}\begin{bmatrix}m_e\end{bmatrix} + \begin{bmatrix}0\\ \frac{-1}{T_2}\\ 0\end{bmatrix}\begin{bmatrix}m_L\end{bmatrix}, \tag{1}$$

where: ω_1, ω_2 – the speeds of the motor and load side, respectively, m_e, m_s, m_L – the electromagnetic, coupling (shaft), and load torques, T_1, T_2 – the mechanical time constant of the motor and load side, T_c – the parameter which represents the elasticity of the coupling.

Figure 1 shows a diagram of the drive system with flexibility. The first mass represents the time constant of the driving motor T_1. The time constant of the load machine is presented analogously on the other side and is denoted as T_2. A flexible shaft with the main parameter stiffness time constant T_c connects both masses.

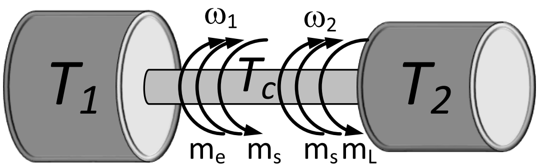

Fig. 1. Schematic diagram of two-mass mechanical system

2.2. Control structure

Due to the elasticity of the mechanical connection, the speed of the driving motor is different from the speed of the load machine during transients. It results in torsional vibrations that are undesirable from the point of view of control quality and durability of the system. To minimize this effect and preserve the high dynamic of the drive, one of the advanced control structures should be implemented [1, 2, 4–8]. The considered control structure is presented in Fig. 2.

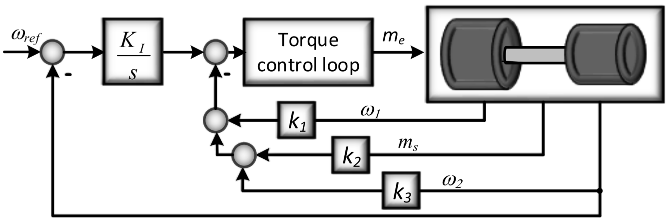

Fig. 2. Block diagram of the considered control system

It consists of two main control loops. In the inner loop, a suitable control method is implemented to ensure fast torque control (e.g., current controller for DC motor or DTC for induction machine). Therefore, the dynamic of this loop is usually neglected for further analysis. In the outer loop, the state controller is considered in the present studies. The parameters of the state controller are set with the use of the pole-placement method, according to the following formulas equations (2)–(5):

$$K_I = T_1 T_2 T_c \omega_r^4, \tag{2}$$

$$k_1 = 4T_1\xi_r\omega_r, \tag{3}$$

$$k_2 = T_1 T_c\left(2\omega_r^2 + 4\xi_r^2\omega_r^2 - \frac{1}{T_2 T_c} - \frac{1}{T_1 T_c}\right), \tag{4}$$

$$k_3 = k_1\left(\omega_r^2 T_2 T_c - 1\right), \tag{5}$$

where: ω_r, ξ_r – the desired frequency and damping coefficient of the system poles (close-loop).

The presented formulas allow for locating the system closed-loop poles into the desired position in the plane. Therefore, in a linear range of work, different shapes of controlled states can be obtained.

This control structure requires knowledge of the two-mass system parameters (T_1, T_2, and T_c). Time constant T_1 can be calculated based on motor datasheets. The other two parameters depend on the type of coupling and load machine and can vary during system operation. Therefore, an application of the special identification scheme is required. In the work, a solution based on fuzzy MKF is proposed.

3. MULTI-LAYER EKF-BASED ESTIMATOR

3.1. Extended Kalman filter

To estimate the unknown value of T_2 and T_c, the original state vector of the system has to be extended to [15]:

$$\mathbf{x_R}(t) = \left[\omega_1(t)\ \ \omega_2(t)\ \ m_s(t)\ \ \frac{1}{T_2}(t)\ \ \frac{1}{T_c}(t)\right]^T. \tag{6}$$

It should be emphasized that (6) cannot be further extended by load torque due to observability conditions.

The state equations are taking following forms:

$$\begin{aligned}\dot{\mathbf{x}}_\mathbf{R}(t) &= \mathbf{A_R}\left(\frac{1}{T_2}(t), \frac{1}{T_c}(t)\right)\mathbf{x_R}(t) + \mathbf{B_R}\mathbf{u}(t) + \mathbf{w}(t) \\ &= \mathbf{f_R}\left(\mathbf{x_R}(t), \mathbf{u}(t)\right) + \mathbf{w}(t), \end{aligned}\tag{7}$$

$$\mathbf{y_R}(t) = \mathbf{C_R}\mathbf{x_R}(t) + \mathbf{v}(t), \tag{8}$$

where: $\mathbf{w}(t)$ – process error, $\mathbf{v}(t)$ – measurement error.

The state, and output matrices are defined as equation (9):

$$\mathbf{A_R}\left(\frac{1}{T_2}(t), \frac{1}{T_c}(t)\right) = \begin{bmatrix} 0 & 0 & \frac{-1}{T_1} & 0 & 0 \\ 0 & 0 & \frac{1}{T_2(t)} & 0 & 0 \\ \frac{1}{T_c(t)} & \frac{-1}{T_c(t)} & 0 & 0 & 0 \\ 0 & 0 & 0 & 0 & 0 \\ 0 & 0 & 0 & 0 & 0 \end{bmatrix},$$
$$\mathbf{B_R} = \left[\frac{1}{T_1}\ 0\,0\,0\,0\right], \qquad \mathbf{C_R} = \left[1\ \ 0\ \ 0\ \ 0\ \ 0\right]^T. \tag{9}$$

Parameters T_2 and T_c evident in matrix $\mathbf{A_R}$ can be changeable during the estimation process. It means that this matrix must be updated in every calculation step. To compute these calculations, the linearization process must be performed. The discretized state equations can be formulated as equation (10):

$$\begin{aligned}\hat{x}_\mathbf{R}(k+1|k+1) &= \hat{x}_\mathbf{R}(k+1|k) \\ &+ \mathbf{K}(k+1)\left[\mathbf{y_R}(k+1) - \mathbf{C_R}\hat{x}_\mathbf{R}(k+1|k)\right].\end{aligned} \tag{10}$$

The gain matrix $\mathbf{K}$ is obtained using the following numerical procedure. First, the state vector predictor is calculated:

$$\mathbf{P}(k+1|k) = \mathbf{F_R}(k)\mathbf{P}(k)\mathbf{F}_\mathbf{R}^T(k) + \mathbf{Q}(k), \tag{11}$$

where:

$$\mathbf{F_R}(k) = \left.\frac{\partial \mathbf{f_R}\left(\mathbf{x_R}(k|k),\ \mathbf{u}(k|k),\ k)\right)}{\partial \mathbf{x_p}(k|k)}\right|_{\mathbf{x_R}=\hat{\mathbf{x}}_\mathbf{R}(k|k)}. \tag{12}$$

$\mathbf{F_R}$ is the linearized state matrix of the system equation (11), which is updated in every calculation step according to the sampling period T_p:

$$\mathbf{F_R} = \begin{bmatrix} 1 & 0 & \frac{-T_p}{T_1} & 0 & 0 \\ 0 & 1 & \frac{T_p}{T_2(k)} & T_p m_s(k) & 0 \\ \frac{T_p}{T_c(k)} & \frac{-T_p}{T_c(k)} & 1 & 0 & T_p\left[\omega_1(k) - \omega_2(k)\right] \\ 0 & 0 & 0 & 1 & 0 \\ 0 & 0 & 0 & 0 & 1 \end{bmatrix}. \tag{13}$$

The gain matrix $\mathbf{K}$ and predictor $\mathbf{P}$ are calculated according to equations (14)–(15):

$$\mathbf{K}(k+1) = \mathbf{P}(k+1|k)\mathbf{C}_\mathbf{R}^T\left[\mathbf{C_R}\mathbf{P}(k+1|k)\mathbf{C}_\mathbf{R}^T + a\mathbf{R}(k)\right]^{-1}, \tag{14}$$

$$\mathbf{P}(k+1|k+1) = \left[\mathbf{I} - \mathbf{K}(k+1)\mathbf{C_R}\right]\mathbf{P}(k+1|k). \tag{15}$$

This section shows the standard algorithm of EKF used for the simultaneous estimation of two-mass system parameters T_2 and T_c. The convergence of estimated states depends on the parameters of the covariance matrices. To ensure the stable operation of the estimator, these values are limited. To speed up the estimation process and improve the accuracy of the estimated states, the fuzzy MKF is proposed in the paper.

3.2. Multi-layer EKF

In the paper, a multi-layer estimator is considered. In the first one, some numbers (here three) of the single EKF are placed. They are supplied with identical signals: electromagnetic torque and motor speed. The filters have identical parameters ($\mathbf{Q}$, $\mathbf{R}$), yet they are working separately. The difference lies in the initial conditions of the states. Different initial values of the estimated parameters are placed here (T_2 and T_c). These conditions can be further extended by setting initial values of other states: e.g. shaft torque resulting from an initial twist of the joint. In the second layer, an aggregation mechanism based on historical samples of the estimation error of driving speed is implemented. It connects the incoming states from a single EKF and generates the final output of the system. The following formula is implemented for this purpose:

$$\mathbf{x} = \alpha_1\mathbf{x}_1 + \alpha_2\mathbf{x}_2 + \alpha_3\mathbf{x}_3\,, \tag{16}$$

where: $\mathbf{x}$ – final state vector of MKF, $\mathbf{x}_1 - \mathbf{x}_3$ – state vectors of particular EKF, $\alpha_1 - \alpha_3$ are normalized coefficients.

As can be concluded from the above equation, the larger the coefficient, the greater the impact of a given estimator on the output signal. The α coefficients are calculated in the two-step procedure, shown in Fig. 3. Firstly based on the estimation error

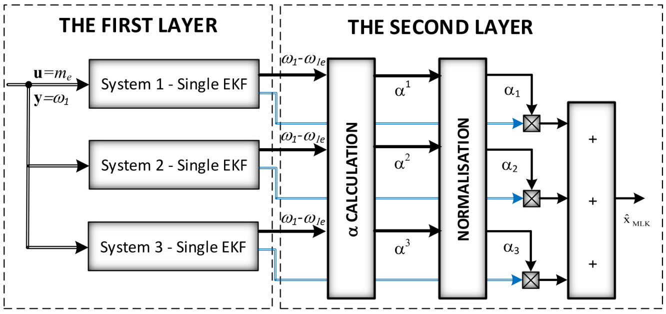

Fig. 3. Block diagram of MKF

of each EKF in the first layer, absolute values α^n (Fig. 3) are determined:

$$\alpha^n = \frac{1}{\gamma \int |\omega_{1m} - \widehat{\omega}_{1n}| \, \mathrm{d}t}, \tag{17}$$

where: ω_{1m} – measured motor speed, $\widehat{\omega}_{1n}$ – motor speed estimated by n-th EKF, γ – learning coefficient.

Then the normalization procedure is applied to determine the coefficient α_n (Fig. 3) values for each EKF:

$$\alpha_n = \frac{\alpha^n}{\sum_{i=1}^{n} \alpha^i}. \tag{18}$$

In order to meet the following condition:

$$\alpha_1 + \alpha_2 + \alpha_3 = 1. \tag{19}$$

In the following procedure, values α are influenced by all samples from starting point of the algorithm.

It should be emphasized that the multi-layer concept does not depend on guessing the initial condition of the system. The main idea relies on the implementation of a special aggregation mechanism based on historical samples laying inside a past window with the length depending on the forgetting factor. The block diagram of MKF is presented in Fig. 3.

3.3. Fuzzy type II system

Preliminary studies of such an algorithm are presented in the conference paper [30] (some results will also be placed in the results section). The main drawback is disruptions evident in estimated transients. They result from the non-zero friction torque evident in a real system. The load (friction) torque cannot be included in the algorithm due to the observability condition of the plant. To improve the performance of the estimator, an additional solution is proposed here. The estimation of the system parameters is only possible during the dynamic state of the plant (changeable value of the motor speed and driving torque) [15]. The disruption is significant when the motor speed has a constant value. Therefore, in this paper, an additional system (detection system) that switches on and off the updating of the states in the estimation mechanism is proposed.

The detection system is based on three signals: motor speed, driving torque, and the difference between the driving and shaft torques – those signals create an input vector of the fuzzy system. Then the incoming signals are fuzzed with the help of triangular II types sets. The output of membership functions has two values, determined by the upper and lower boundaries. It further creates two groups of premises, the t-norm *min* is used to determine firing levels of rules according to expressions like equation (20):

$$R^3_{\max} = \min\left[\mu^1_{P\max}(m_e(k)),\ \mu^2_{P\max}(m_e(k) - m_{se}(k)),\ \mu^3_{N\max}(\Delta\omega_1(k))\right]. \tag{20}$$

Each rule firing level is multiplied by an adequate gain coefficient corresponding with the number of positive membership functions involved in a given rule. In the end, the reduction type block is applied. The system has 16 rules. The schematic block of the fuzzy detection system is shown in Fig. 4.

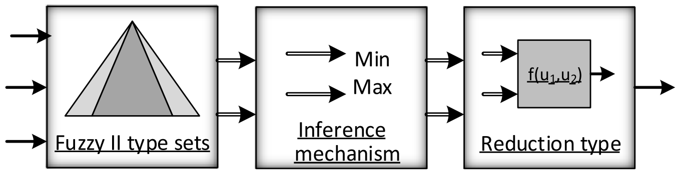

Fig. 4. Schematic block diagram of the fuzzy detection

4. RESULTS

The proposed fuzzy MKF is tested under a variety of simulation and experimental tests. The transients from the following system are additionally presented: single EKFs and MKF [30], which will facilitate the evaluation of the effectiveness of the proposed approach. The difference between MKF and fuzzy MKF relies on the implementation of a detection system. The other parameters in both structures remain identical.

The tested system works under reverse conditions. The reference value of the system speed is set to 0.5 with a frequency of 0.5 Hz. The values of **Q** and **R** matrices in a single KF are chosen experimentally. Initial states of each EKF system and each T_2, T_c estimation signal filter was chosen experimentally from the range of values 0.01–1 for T_2 and 0.0001–0.01 for T_c, assuming that two are close to the set borders. The parameters of the state recognition system are selected experimentally. The system with unknown values of T_2 and T_c is tested. Then at the time $t = 10$ s an increase of 50% for T_2 is considered.

The results of the simulation studies are shown in Fig. 5. The input signals for multi-observer are – motor speed (Fig. 5a) and driving torque (Fig. 5b). The transients of estimated values of T_2 and T_c are shown in Fig. 5c–d, and their enlargement in Fig. 5e, f. The variations of weights coefficients α_1–α_3 are demonstrated in Fig. 5g and the output of the fuzzy detection system is in Fig. 5h.

The following remarks can be formulated based on the presented results. The accuracy of the single EKF depends strictly on the set initial values. The nearer those values are, the smaller estimation errors are evident. However, it also has a drawback which is visible in Fig. 5c–f. The estimation of T_2 and T_c is possible only dynamic states of the plant. Under different conditions, due to the non-zero friction torque, the triangular-shaped

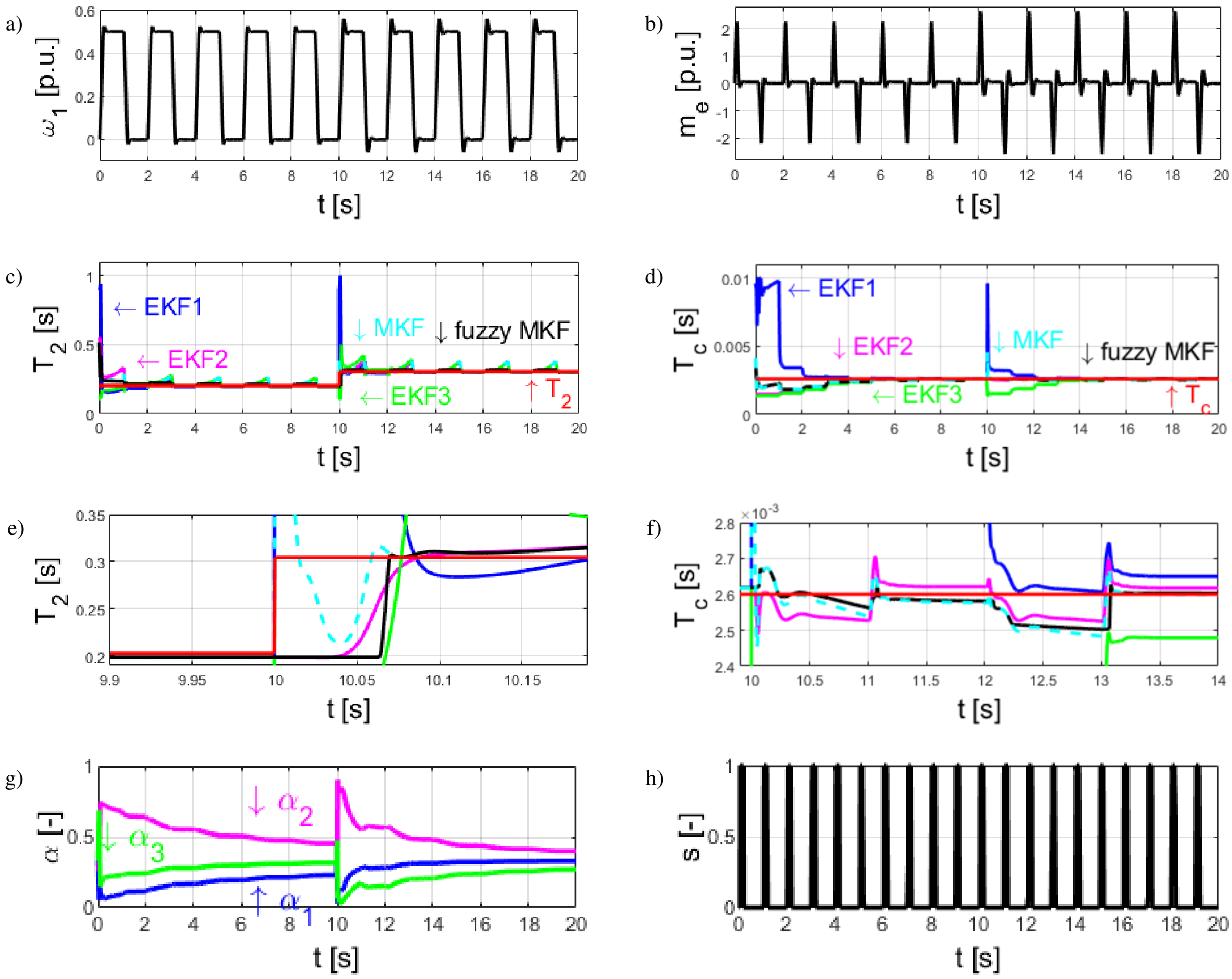

Fig. 5. Transients of the motor speed ω_1 (a); and driving torque m_e (b); estimated values of the time constant of load machine T_2 (c),(e); elasticity time constant T_c (d),(f); weight coefficients (g), and output detection system (h)

disruption is visible in estimated T_2 transients. To eliminate it, the fuzzy MKF is proposed. The detection system identifies the present state in a plant – its output is shown in Fig. 5h. During dynamic state, the updating in system states is switched on, otherwise off. The transients of the estimated parameters provided by fuzzy MKF are presented (black lines) in Fig. 5c–f (only output of the system –not single EKF). Moreover, Fig. 5c–f shows that the fuzzy MKF system responds most quickly to the change of parameters. The improvement of estimated states is visible. The estimated values converge around the real values evident in the plant.

The variation of coefficients is shown in Fig. 5g. The times, when the system is switched off, are visible in its transients. To evaluate the properties of considered systems, the estimation errors are computed using the following equations:

$$\Delta_E = \frac{\sum_{i=1}^{N} |v - v_e|}{N}, \tag{21}$$

where: N – total number of samples, v – real variable, v_e – estimated variable.

$$\Delta_E = \frac{\Delta_E}{\Delta_{f\mathrm{MKF}}} \times 100\%, \tag{22}$$

where: $\Delta_{f\mathrm{MKF}}$ errors for fuzzy MKF.

In Table 1 the estimation errors calculated from the simulation test are presented. Three systems are compared in Table 1: the classical EKF (system with three different parameters indicated: EKF 1, EKF 2, and EKF 3), the MKF algorithm described in [30], and the fuzzy MKF proposed in this paper. When comparing the two most advanced algorithms, the estimation errors in the MKF algorithm are larger by 67 percentage points for T_2 and 5 percentage points for T_c. It is visible that the implementation of the fuzzy detection system reduces the estimation error in T_2 significantly. It should be also stated that single EKFs have much bigger errors in all estimated variables.

Then, experimental studies are performed. The considered estimators are tested on a stand built of two 500 W DC motors

Table 1

Simulation test – estimation errors of the single EKF algorithms, previously presented MKF algorithm and its extension presented in this paper – fuzzy MKF

	EKF 1 Δ [–]	EKF 2 Δ [–]	EKF 3 Δ [–]	MKF Δ [–]	fuzzy MKF Δ [–]
ω_1	4.015e–4	3.12e–4	3.755e–4	3.041e–4	3.041e–4
ω_2	5e–3	2.9e–3	3.7e–3	3e–3	3e–3
m_s	1.11e–2	8.8e–3	1.18e–2	8e–3	8e–3
T_2	2.13e–2	2.02e–2	1.98e–2	1.76e–2	1.05e–2
T_c	4.933e–4	1.934e–4	3.294e–4	1.47e–4	1.401e–4
	δ [%]	δ [%]	δ [%]	δ [%]	δ [%]
ω_1	132	103	123	100	100
ω_2	168	98	126	100	100
m_s	138	110	147	100	100
T_2	202	191	187	167	100
T_c	352	138	235	105	100

connected by a flexible shaft. It is shown in Fig. 6. The driving motor is operated by a power converter which is controlled by the dSPACE controller board. The laboratory equipment facilitates the measurement of both motor speeds and driving motor currents.

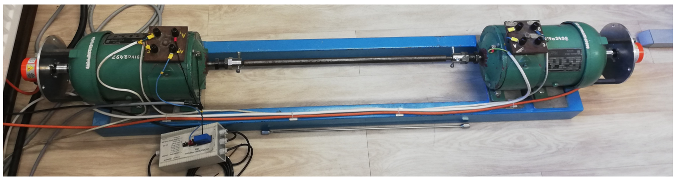

Fig. 6. Photo of the laboratory set-up

Firstly, the observer is working in an open-loop system. That means that the motor speed (Fig. 7a) and driving torque (Fig. 7b) are collected and then supplied MKF. The transients of the estimated variables are presented in Fig. 7c–d.

In Figure 7c–d transients taken from a single EKF are presented. It is visible that during steady-state the values of T_2 are increasing significantly, due to the existence of the friction torque. To clarify of presentation, the transients of MKF are not included in the picture. After a few periods, it will cover the green line exactly. The only output of fuzzy MKF is included in the figures. It is seen that the presented transients possessed small estimation errors.

Next, the properties of the adaptive system working with single EKF and fuzzy MKF are evaluated. It means that the control structure coefficients (Fig. 2) are returned according to identified values of estimated parameters provided by fuzzy MKF. The feedback in the state controller comes also from the esti-

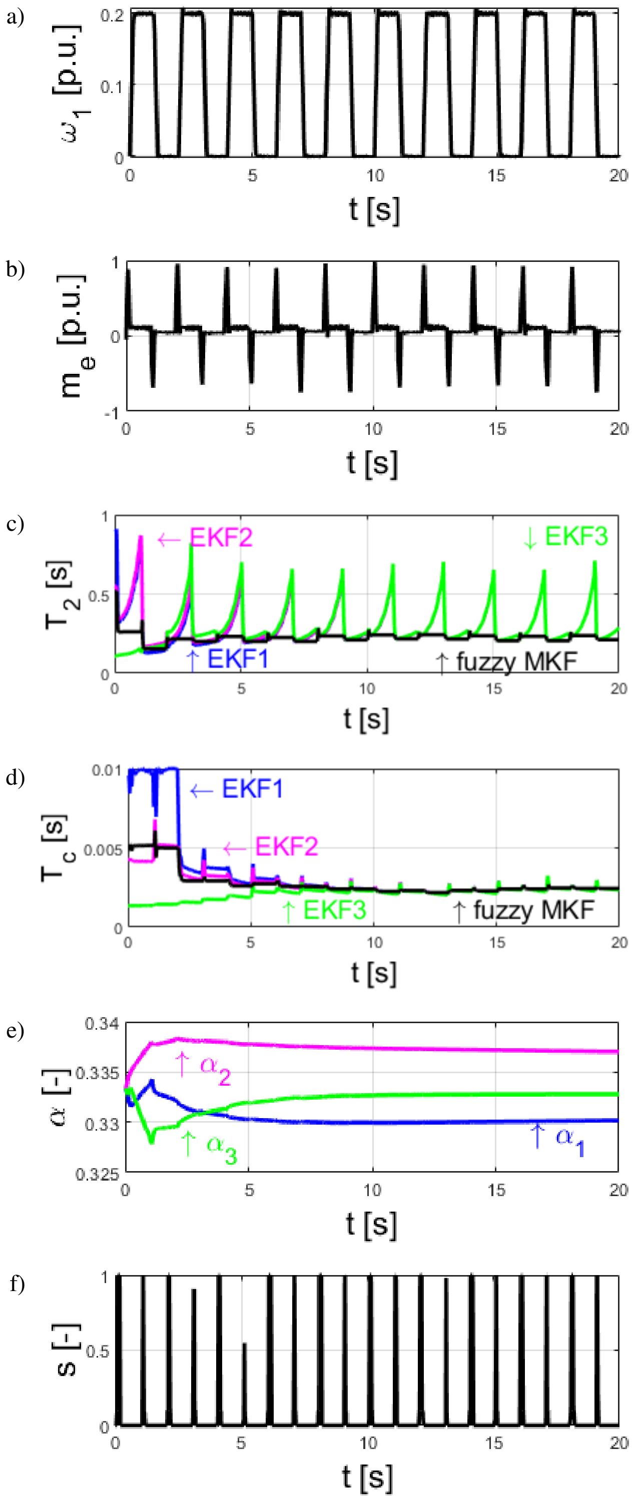

Fig. 7. Experimental results: a), b) – the transients of the driving motor speed ω_1 and electromagnetic torque m_e, c), d), – the transients of the T_2, T_c parameters identification with close-ups, e) – the transients of weight coefficients, f) – the transient of the state recognition system output signal

mator. The initial values of the system parameters for EKF are selected as: $T_2 = 0.892$ [s] and $T_c = 0.0096$ [s]. In the case of fuzzy MKF, the initial parameters for the next two single observers are: $T_{22} = 0.5517$ [s]; $T_{c2} = 0.0043$ [s]; $T_{23} = 0.106$ [s]; $T_{c3} = 0.0013$ [s]. Firstly, the system working with a single EKF is tested. The motor and load speeds are presented in Fig. 8a as well as motor and shaft torques in Fig. 8b. Since initial system mechanical parameters are not set properly, the system closed-loop poles are far away from the desired position. It results in large oscillations in speeds and torques. The driving torque is limited to the value of 3 [p.u.] to protect the shaft. Also, the shaft torque exceeded the value of 3. Both speeds had large overshoots more than 150%. After one period of work, those oscillations are drastically reduced. Still, some disruptions are visible in system states. The transients for a system with fuzzy MKF are presented in Fig. 8a,b. In the driving torques, oscillations are also visible, yet they are much smaller than in the previously considered case. The maximum value of this variable is 1.8 [p.u.] The shaft torque has smooth transients. The overshoot in system speed is about 50%. After one period of work shape, all transients are smooth, and no oscillations are visible.

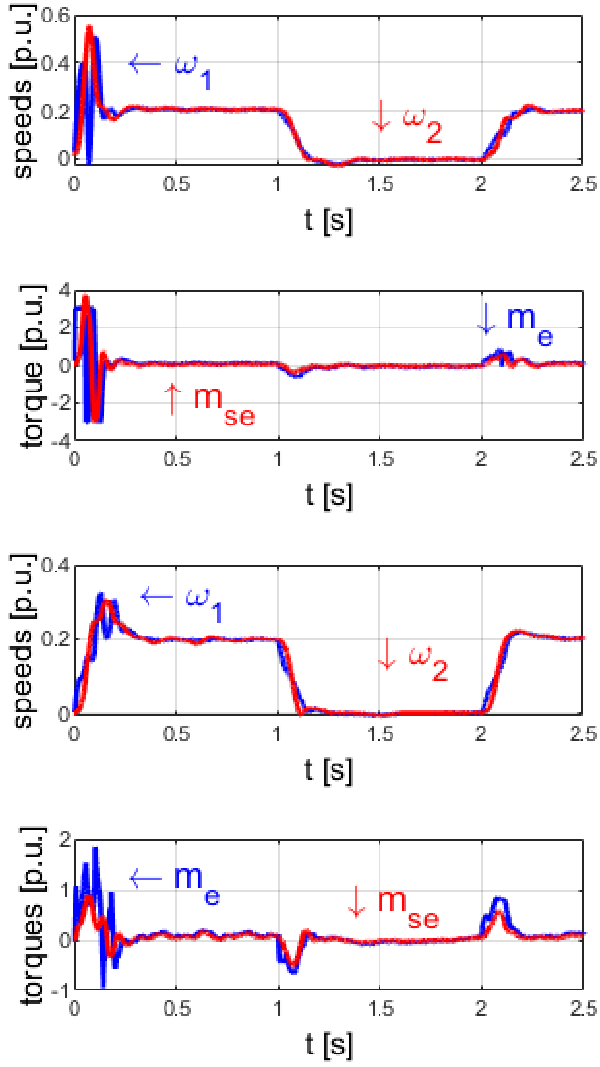

Fig. 8. Transients from the adaptive control system: the motor ω_1 and load ω_2 speeds a), c) driving m_e, and shaft torque m_s in the system working with single EKF a)–b) and working with fuzzy MKF c)–d)

5. CONCLUSIONS

In the paper, issues related to the application of the online identification scheme for a two-mass drive system are presented. As an identification algorithm, a fuzzy MKF is selected. It is based on the multi-layer concept consisting of two parts and an additional fuzzy II type system. In the first part, three single EKFs are placed, and in the second, an aggregation mechanism is implemented. The fuzzy system is used to detect the current state of the plant and switch on or off the identification algorithm. Based on the theoretical consideration and tests, the following remarks can be formulated. To calculate the gains of an advanced control structure, knowledge of the plant parameters is necessary. The solution based on EKF can be used to determine the values of the stiffness and load machine time constants. However, the accuracy of EKF is greatly influenced by the initial values of those parameters that can be unknown. To shorten the convergence time of system states the multi-layer concept can be used. However, in the considered case, due to the observability conditions, the existing load torque (friction torque) cannot be included in the state matrix.

This factor causes slowly increasing errors in the estimated values of the plant parameters during steady-state. To eliminate this effect, an additional fuzzy system is proposed. It determines the present state of the plant: dynamic or static and switches the estimation algorithm on or off. The use of type II membership functions in fuzzy state detection blocks ensures the high reliability of this system. The fuzzy MKF is also tested in a closed-loop system where the present values of the estimated T_2 and T_c retune the control structure gains. This system ensures better properties of the plant as compared to the classical EKF. The overshoots and oscillations possess a smaller value in this system.

REFERENCES

[1] S. Brock, D. Łuczak, K. Nowopolski, T. Pajchrowski, and K. Zawirski, "Two Approaches to Speed Control for Multi-Mass System with Variable Mechanical Parameters," *IEEE Trans. Ind. Electron.*, vol. 64, pp. 3338–3347, 2016.

[2] P. Serkies, "Estimation of state variables of the drive system with elastic joint using moving horizon estimation (MHE)," *Bull. Pol. Acad. Sci. Tech. Sci.*, vol. 67, no. 5, pp. 883–892, 2019.

[3] M. Iwasaki, K. Seki, and Y. Maeda, "High-Precision Motion Control Techniques: A Promising Approach to Improving Motion Performance," *IEEE Ind. Electron. Mag.*, vol. 6, no. 1, pp. 32–40, Mar. 2012, doi: 10.1109/MIE.2012.2182859.

[4] M. Ruderman, M. Iwasaki, and W. Chen, "Motion-control techniques of today and tomorrow: a review and discussion of the challenges of controlled motion," *IEEE Ind. Electron. Mag.*, vol. 14, no. 1, pp. 41–55, Mar. 2020, doi: 10.1109/MIE.2019.2956683.

[5] J. Kabziński and P. Mosiołek, "Integrated, Multi-Approach, Adaptive Control of Two-Mass Drive with Nonlinear Damping and Stiffness," *Energies*, vol. 14, p. 5475, 2021.

[6] R. Szczepanski, M. Kaminski, and T. Tarczewski, "Auto-Tuning Process of State Feedback Speed Controller Applied for Two-Mass System," *Energies*, vol. 13, p. 3067 2020.

[7] S.E. Saarakkala and M. Hinkkanen, "Identification of Two-Mass Mechanical Systems Using Torque Excitation: Design and Experimental Evaluation," *IEEE Trans. Ind. Appl.*, vol. 51, no. 5, pp. 4180–4189, Sep./Oct. 2015, doi: 10.1109/TIA.2015.2416128.

[8] M. Östring, S. Gunnarsson, and M. Norrlöf, "Closed-loop identification of an industrial robot containing flexibilities," *Control Eng. Pract.*, vol. 11, no. 3, pp. 291–300, Mar. 2003.

[9] S.-M. Yang and S.-C. Wang, "The detection of resonance frequency in motion control systems," *IEEE Trans. Ind. Appl.*, vol. 50, no. 5, pp. 3423–3427, Sep./Oct. 2014.

[10] Y. Yoshioka and T. Hanamoto, "Estimation of a multimass system using the LWTLS and a coefficient diagram for vibration-controller design," *IEEE Trans. Ind. Appl.*, vol. 44, no. 2, pp. 566–574, Mar./Apr. 2008.

[11] S. Villwock and M. Pacas, "Application of the Welch-method for the identification of two- and three-mass-systems," *IEEE Trans. Ind. Electron.*, vol. 55, no. 1, pp. 457–466, Jan. 2008.

[12] D. Łuczak, "Nonlinear Identification with Constraints in Frequency Domain of Electric Direct Drive with Multi-Resonant Mechanical Part," *Energies* vol. 14, no. 21, p. 7190, 2021, doi: 10.3390/en14217190.

[13] J.-H. Montonen, N. Nevaranta, T. Lindh, J. Alho, P. Immonen, and O. Pyrhonen, "Experimental Identification and Parameter Estimation of the Mechanical Driveline of a Hybrid Bus," *IEEE Trans. Ind. Electron.*, vol. 65, pp. 5921–5930, 2018.

[14] N. Nevaranta, J. Parkkinen, T. Lindh, M. Niemelä, O. Pyrhönen, and J. Pyrhönen, "Online Estimation of Linear Tooth Belt Drive System Parameters," *IEEE Trans. Ind. Electron.*, vol. 62, no. 11, pp. 7214–7223, Nov. 2015, doi: 10.1109/TIE.2015.2432103.

[15] K. Szabat and T. Orlowska-Kowalska, "Application of the Kalman filters to the high-performance drive system with elastic coupling," *IEEE Trans. Ind. Electron.*, vol. 59, no. 11, pp. 4226–4235, Nov. 2012.

[16] M. Perdomo, M. Pacas, T. Eutebach, and J. Immel, "Sensitivity analysis of the identification of variable inertia with an extended kalman filter," *Proc. IEEE IECON*, Nov. 2013, pp. 3102–3107.

[17] K. Szabat and T. Orlowska-Kowalska, "Vibration Suppression in Two-Mass Drive System using PI Speed Controller and Additional Feedbacks – Comparative Study," *IEEE Trans. Ind. Electron.*, vol. 54, no. 2, pp. 1193–1206, Apr. 2007, doi: 10.1109/TIE.2007.892608.

[18] S. Katsura and K. Ohnishi, "Force Servoing by Flexible Manipulator Based on Resonance Ratio Control," *IEEE Trans. Ind. Electron.*, vol. 54, no. 1, pp. 539–547, Feb. 2007.

[19] H. Kobayashi, S. Katsura, and K. Ohnishi, "An Analysis of Parameter Variations of Disturbance Observer for Motion Control," *IEEE Trans. Ind. Electron.,* vol. 54, no. 6, pp. 3413–3421, Dec. 2007.

[20] S. Katsura, J. Suzuki, and K. Ohnishi, "Pushing Operation by Flexible Manipulator Taking Environmental Information Into Account," *IEEE Trans. Ind. Electron.*, vol. 53, no. 5, pp. 1688–1697, Oct. 2006.

[21] J. Kabziński and P. Mosiołek, "Adaptive, nonlinear state transformation-based control of motion in presence of hard constraints," *Bull. Pol. Acad. Sci. Tech. Sci.*, vol. 68, no. 5, pp. 963–971, 2020.

[22] M. Zychlewicz, R. Stanislawski, and M. Kaminski, "Grey Wolf Optimizer in Design Process of the Recurrent Wavelet Neural Controller Applied for Two-Mass System," *Electronics*, vol. 11, p. 177, 2022, doi: 10.3390/electronics11020177.

[23] K. Szabat and T. Orlowska-Kowalska, "Performance Improvement of Industrial Drives With Mechanical Elasticity Using Nonlinear Adaptive Kalman Filter," *IEEE Trans. Ind. Electron.*, vol. 55, no. 3, pp. 1075–1084, March 2008.

[24] M. Cychowski, K. Szabat, and T. Orlowska-Kowalska, "Constrained Model Predictive Control of the Drive System With Mechanical Elasticity," *IEEE Trans. Ind. Electron.*, vol. 56, no. 6, pp. 1963–1973, June 2009, doi: 10.1109/TIE.2009.2015753.

[25] C. Wang, M. Yang, W. Zheng, J. Long, and D. Xu, "Vibration Suppression With Shaft Torque Limitation Using Explicit MPC-PI Switching Control in Elastic Drive Systems," *IEEE Trans. Ind. Electron.*, vol. 62, no. 11, pp. 6855–6867, Nov. 2015.

[26] M. Yang, C. Wang, D. Xu, W. Zheng, and X. Lang, "Shaft Torque Limiting Control Using Shaft Torque Compensator for Two-Inertia Elastic System With Backlash," *IEEE/ASME Trans. Mechatron.*, vol. 21, no. 6, pp. 2902–2911, Dec. 2016.

[27] P. Serkies and A. Gorla, "Implementation of PI and MPC-Based Speed Controllers for a Drive with Elastic Coupling on a PLC Controller," *Electronics*, vol. 10, p. 3139, 2021, doi: 10.3390/electronics10243139.

[28] B. Firouzi *et al*., "A Type-2 Fuzzy Controller for Floating Tension-Leg Platforms in Wind Turbines," *Energies*, vol. 15, p. 1705, 2022, doi: 10.3390/en15051705.

[29] P. Derugo, K. Szabat, T. Pajchrowski, and K. Zawirski, "Fuzzy Adaptive Type II Controller for Two-Mass System," *Energies*, vol. 15, p. 419, 2022, doi: 10.3390/en15020419.

[30] K. Śleszycki, K. Wróbel, K. Szabat, and S. Katsura, "Parameter Identification of the Two-Mass System with the help of Multilayer Estimator," *2021 IEEE Int. Symp. Ind. Electron., (ISIE)*, 2021, pp. 1–6, doi: 10.1109/ISIE45552.2021.9576313.

[31] K. Szabat, K. Wróbel, and S. Katsura, "Application of Multilayer Kalman Filter to a Flexible Drive System," *IEEJ J. Ind. Appl.*, vol. 11, no. 3, pp. 483–493, 2022, doi: 10.1541/ieejjia.21009655.

[32] J. Bernat, J. Kolota, P. Superczynska, and S. Stepien, "Multilayer observer as new structure for state estimation in linear systems," *Arch. Electr. Eng.*, vol. 66, no. 3, pp. 507–521, 2017.